Accurate machine-specific reference and small-field dosimetry for a self-shielded neuro-radiosurgical system

Jermain, Peter R.; Muir, Bryan; McEwen, Malcolm; Niu, Ying; Pang, Dalong

Publisher's version / Version de l'éditeur:
https://doi.org/10.1002/mp.17111
Medical Physics, 51, 6, pp. 4423-4433, 2024-05-02

Received: 5 January 2024 | Revised: 14 March 2024 | Accepted: 18 April 2024

DOI: 10.1002/mp.17111

RESEARCH ARTICLE

MEDICAL PHYSICS

Accurate machine-specific reference and small-field dosimetry for a self-shielded neuro-radiosurgical system

Peter R. Jermain[1] | **Bryan Muir**[2] | **Malcolm McEwen**[2] | **Ying Niu**[1] | **Dalong Pang**[1]

[1]Department of Radiation Medicine, Medstar Georgetown University Hospital, Washington, District of Columbia, USA

[2]Metrology Research Centre, National Research Council, Ottawa, Ontario, Canada

Correspondence
Dalong Pang, 3800 Reservoir Road NW, Lower Level (LL) Bles Bldg, Washington, DC 20007, USA.
Email: pangd@georgetown.edu

Abstract

Background: The newly available ZAP-X stereotactic radiosurgical system is designed for the treatment of intracranial lesions, with several unique features that include a self-shielding, gyroscopic gantry, wheel collimation, non-orthogonal kV imaging, short source-axis distance, and low-energy mega-voltage beam. Systematic characterization of its radiation as well as other properties is imperative to ensure its safe and effective clinical application.

Purpose: To accurately determine the radiation output of the ZAP-X with a special focus on the smaller diameter cones and an aim to provide useful recommendations on quantification of small field dosimetry.

Methods: Six different types of detectors were used to measure relative output factors at field sizes ranging from 4 to 25 mm, including the PTW microSilicon and microdiamond diodes, Exradin W2 plastic scintillator, Exradin A16 and A1SL ionization chambers, and the alanine dosimeter. The 25 mm cone served as the reference field size. Absolute dose was determined with both TG-51-based dosimetry using a calibrated PTW Semiflex ion chamber and measurements using alanine dosimeters.

Results: The average radiation output factors (maximum deviation from the average) measured with the microDiamond, microSilicon, and W2 detectors were: for the 4 mm cone, 0.741 (1.0%); for the 5 mm cone: 0.817 (1.0%); for the 7.5 mm cone: 0.908 (1.0%); for the 10 mm cone: 0.946 (0.4%); for the 12.5 mm cone: 0.964 (0.2%); for the 15 mm cone: 0.976 (0.1%); for the 20 mm cone: 0.990 (0.1%). For field sizes larger than 10 mm, the A1SL and A16 micro-chambers also yielded consistent output factors within 1.5% of those obtained using the microSilicon, microdiamond, and W2 detectors. The absolute dose measurement obtained with alanine was within 1.2%, consistent with combined uncertainties, compared to the PTW Semiflex chamber for the 25 mm reference cone.

Conclusion: For field sizes less than 10 mm, the microSilicon diode, micro-Diamond detector, and W2 scintillator are suitable devices for accurate small field dosimetry of the ZAP-X system. For larger fields, the A1SL and A16 micro-chambers can also be used. Furthermore, alanine dosimetry can be an accurate verification of reference and absolute dose typically measured with ion chambers. Use of multiple suitable detectors and uncertainty analyses were recommended for reliable determination of small field radiation outputs.

KEYWORDS
radiosurgery, small field dosimetry, ZAP-X

1 | INTRODUCTION

Stereotactic radiosurgery (SRS) has been increasingly utilized for management of intracranial brain lesions during the last decades.[1,2] This technique delivers a high dose of precisely targeted radiation to the treatment site over a limited number of fractions (typically between one and five),[3] and provides effective tumor control, minimizes radiation to healthy tissues, and reduces overall duration of treatment.[4] Several studies have demonstrated greater therapeutic benefits from SRS versus whole brain radiotherapy (WBRT) or partial brain radiotherapy (PBRT) for the treatment of benign and malignant primary brain tumors and brain metastases.[5–7] In addition, SRS is associated with fewer neurological toxicities or poor cognitive outcomes (e.g., memory loss and emotional dysfunction) as compared to WBRT.[8–10]

Radiosurgery was ushered in with the development of Gamma Knife by Swedish neurosurgeon Lars Leksell in 1968. Designed as a tool for treatment of deep-seated neoplasms and vascular disorders of the brain, the first Gamma Knife unit focused radiation from 179 cobalt-60 sources to a single point in the brain to treat diseases.[11] In the early 1990s, the first linear accelerator-based SRS system at University of Florida incorporated a design with precision bearings to achieve desired targeting accuracy.[12] Further advances yielded improved immobilization devices, frameless radiosurgery, and tools for precision patient monitoring.[13–15] CyberKnife is another modern SRS system that includes a compact linear accelerator attached to an articulated robotic arm that can provide irradiation from multiple non-coplanar angles.[16] It delivers a 6 MV photon beam using integrated image guidance and fixed cones or variable aperture collimator (IRIS) to enable accurate delivery of high doses of radiation to small, irregular-shaped tumors.[17]

ZAP-X from ZAP Surgical Systems, Inc., is the latest development of radiosurgical systems. A prominent feature of the system is that the treatment vault together with all associated radiation and imaging components are enclosed in a thick steel spherical shell which provides radiation shielding, eliminating the need for construction of a typical vault.[18] Inside the sphere, an S-band linear accelerator mounted on a set of coupled gimbals that rotate on dual axes around the isocenter[19] delivers non-coplanar 2.7 MV photon beams at a maximum dose rate of 1500 monitor units (MU) per min through circular cones as small as 4 mm. Since initial clearance by the Food and Drug Administration in the United States in 2017, ZAP-X has successfully treated over 1000 patients.

Common to all radiosurgical systems, small fields or field segments are used to deliver radiation. Determination of dose for small fields presents a significant technical challenge because of high-dose gradients, lack of charged particle equilibrium, partial occlusion of the radiation source, and detector volume averaging effects.[20] These factors can cause variation in dose measurements (e.g., due to variations in measured output factors) of up to 30%, negatively impacting the overall treatment efficacy and patient safety.[20] To address the issue of accurate and consistent clinical reference dosimetry, several protocols have been developed over the years, including the widely adopted Task Group (TG) report TG-51, its predecessor TG-21, and TG-155 by the American Association of Physicists in Medicine (AAPM), as well as the Technical Report Series (TRS) TRS-398 from the International Atomic Energy Agency (IAEA), and TRS-483, a joint report from the AAPM and IAEA.[21–25] TG-51 is specifically for what are referred to as "standard" radiation fields, but TG-155 and TRS-483 can be applied to small field scenarios. Specific to radiosurgical applications, several investigators have published their research on small field dosimetry.[26–28] However, there is limited agreement about the optimal procedure and/or choice of detector for small field dosimetry of the novel ZAP-X radiosurgery system.

The goals of this study are to (i) validate the reference dose measurement for ZAP-X, (ii) accurately determine ZAP-X radiation output factors using a variety of available detector types and measurement techniques, and (iii) develop a protocol that can be used reliably to characterize small field radiation beam properties. To realize these objectives, we provide a comparison of detector types for output factors determined here for ZAP-X and compare these results to those available in the published literature as well as investigate generalized small-field output factors (e.g., from different radiosurgery treatment machines).

2 | MATERIALS AND METHODS

2.1 | Reference dosimetry

The photon dosimetry formalism of AAPM's TG-51 report uses ionization chambers with a calibration coefficient ($N_{D,w}^{Co-60}$, absorbed-dose-to-water calibration coefficient for a Cobalt-60 beam) traceable to an Accredited Dosimetry Calibration Laboratory (ADCL), which converts the measured signal to an absorbed dose to water by Equation (1):

$$D_w^Q = Mk_Q N_{D,w}^{Co-60} \quad (1)$$

where D_w^Q, M, k_Q, and $N_{D,w}^{Co-60}$ represent absorbed dose to water (Gy), corrected ion chamber reading (C), beam quality conversion factor, and absorbed-dose-to-water calibration coefficient (Gy/C), respectively.[22]

For dose measurements, standard reference conditions prescribed by the TG-51 protocol [e.g., reference depth of 10 cm, source-surface distance (SSD) or source-axis distance (SAD) setup of 100 cm, and field size of 10 cm × 10 cm] cannot be established in ZAP-X, as it uses small circular collimators ranging from 4 to 25 mm in diameter. The TRS-483 code of practice essentially modifies Equation (1) with an additional multiplicative conversion factor to account for the differences in beam geometry (predominantly the field size), $k_{Q_{msr},Q}^{f_{msr},f_{ref}}$, where "msr" and "ref" refer to the machine-specific and reference radiation fields, respectively. We used a reference depth of 7 mm, SSD of 443 mm, and collimator size of 25 mm. The 25 mm diameter cone (largest field size for ZAP-X) is equivalent to a 22.16 mm × 22.16 mm square field, obtained using $R = \frac{4}{\sqrt{\pi}} \frac{A}{P}$, where A and P denote area and perimeter of the corresponding square field size.[29] For this set of conditions and the detectors proposed, the information in TRS-483 indicated that taking $k_{Q_{msr},Q}^{f_{msr},f_{ref}} = 1$ was a reasonable assumption. This effectively reduces the TRS-483 formalism to that of the standard TG-51 formalism routinely used in our clinic, allowing established procedures to be followed. The final step is the selection of k_Q in Equation (1). The ionization chamber chosen for absolute dose measurements was an ADCL calibrated PTW Semiflex ion chamber 31010 (PTW Dosimetry, Freiburg, Germany), as this detector is intended for reference dosimetry of radiotherapy beams.[30] Currently, there is no published data on experimental or Monte-Carlo calculated k_Q factors for the nominal energy of 2.7 MV for this chamber type, and therefore, a value of unity was selected through extrapolation. This was based on the measured value of the beam quality specifier, $\%dd(10\,\text{cm})_X$ for the ZAP-X and the known k_Q response of cylindrical chambers between Co-60 and 6 MV qualities.

2.2 | Radiation source

All measurements presented in this study were performed at MedStar Georgetown University Hospital using the ZAP-X SRS system (ZAP Surgical Systems, Inc., San Carlos, California, USA). The ZAP-X unit utilizes a novel, linear accelerator-based design with a gyroscopic-like gantry supporting both axial and oblique rotation around the isocenter to enable non-coplanar beam delivery. As noted earlier, the 2.7 MV linear accelerator is capable of a 1500 MU/min dose rate, with a SAD of 45 cm. A tungsten wheel collimator (8 circular sizes from 4 to 25 mm defined at the 45 cm isocentric plane) is used to define the field size and a 3 degree of freedom (DOF) table is used for positioning the patient. Following United States FDA approval in 2017, a ZAP-X system was installed at the hospital in 2020 for treatment of intracranial lesions. Initial acceptance testing and commissioning included beam data collection (e.g., PDDs, off-axis ratios, etc.) and absolute output calibrations (based on TG-51), and Imaging and Radiation Oncology Core (IROC) thermoluminescent detector (TLD) protocols.

2.3 | Radiation detectors

Absolute dosimetry was performed using a Semiflex ionization chamber and alanine dosimeters. In addition, six different types of detectors (summarized in Table 1) were used to determine the relative output factors including a microSilicon diode, microDiamond detector, W2 plastic scintillator, A16 and A1SL ionization chambers, and alanine dosimeters.[30–40]

The PTW 60023 microSilicon diode (PTW Dosimetry, Freiburg, Germany) is an unshielded, p-type silicon diode designed to yield high-dose stability, low dose per pulse dependence, and limited sensitivity to temperature variations (usually ≤ 0.1 %/K).[31] The active volume is 0.03 mm^3 with a radius of 0.75 mm and thickness of 18 μm, whereas total dimensions are 7 mm (diameter) and 45.5 mm (length). The detector exhibits a directional response of ≤ 1% for rotation around the chamber axis or tilting the axis up to ± 20°. In addition, no bias voltage is required to operate the microSilicon.

The PTW 60019 solid-state microDiamond detector (PTW Dosimetry, Freiburg, Germany) is a synthetic, single crystal diamond detector that closely approximates radiation response of water (e.g., absorbed dose) at all beam energies.[30,32] It uses an extremely small active volume (0.004 mm^3) and exhibits minimal dependence on temperature (≤ 0.8 %/K) or variation in response based on direction or angle of incidence of the radiation (≤ 1% for ± 20°). The microDiamond is well suited for measurements in fields as small as 4 mm × 4 mm and required no external bias for operation.[28]

Ionization chamber data for output factor measurements was collected using the Exradin A1SL thimble ion chamber and Exradin A16 micro ion chamber (Standard Imaging Inc., Middleton, Wisconsin, USA),[33,34] whereas the PTW 31010 Semiflex ionization chamber (PTW Dosimetry, Freiburg, Germany) was used for absolute dosimetry.[30,35] The A1SL model has a collector diameter of 1.0 mm and length of 4.4 mm. The outer shell diameter is 6.35 mm. The A16 model has a collector diameter of 0.3 mm and length of 1.27 mm, whereas the outside diameter of the shell is 3.4 mm. Collecting volumes for A1SL and A16 devices are 0.053 and 0.007 cm^3, respectively. The Semiflex chamber has a nominal sensitive volume of 0.125 cm^3. All ion chambers were operated at the polarizing voltage of −300 V.

TABLE 1 Characteristics of six detectors used for output factor measurements.

Detector type	Model	Sensitive material	Active volume (mm^3)	Reference point (from manufacturer)
Diode	microSilicon 60023 (PTW Dosimetry)	Silicon	0.03	On diode axis, 0.9 mm from chamber tip
Diode	microDiamond 60019 (PTW Dosimetry)	Synthetic diamond	0.004	On detector axis, 1 mm from detector tip, marked by ring
Plastic scintillator	Exradin W2 (Standard Imaging)	Polystyrene	1.0	Center of the cylindrical volume of the detector and 1.3 mm from the tip
Ionization chamber	Exradin A16 (Standard Imaging)	Gas (air)	7.0	Centroid of collecting volume of the detector
Ionization chamber	Exradin A1SL (Standard Imaging)	Gas (air)	53.0	Centroid of collecting volume of the detector
Alanine dosimeter	Harwell Alanine (Harwell Dosimeters)	L-Alanine	51.0	Center position of the pellet holder

Plastic scintillator measurements were obtained using the Exradin W2 detection system (Standard Imaging Inc., Middleton, Wisconsin, USA).[36] Components include scintillator material that is water equivalent with no temperature, energy, or dose rate dependencies. The W2 detector utilizes a sensitive scintillator (1.0 mm diameter $\times$ 1.0 mm long) encapsulated in a 2.8 mm diameter $\times$ 42 mm long housing, ideal for radiosurgery small field measurements. The scintillating fiber is coupled to an optical fiber (1.0 mm diameter $\times$ 4.0 m long) that transmits light for readout. Exposing the active volume of the W2 to ionizing radiation produces Cherenkov light in addition to scintillation light. Cherenkov radiation occurs when secondary charged particles propagate through the plastic scintillator faster than the phase velocity of light in the transparent medium.[37,38] A correction is applied to separate components of scintillation light from background light in the W2 detector system.

Alanine dosimeters (Harwell Dosimeters Ltd, Didcot, UK) can be used to determine absolute dose traceable to primary standards. When irradiated, alanine dosimeters form stable free radicals (signal decay is $<$ 2% per year) and the dose absorbed is proportional to the concentration of free radicals, which can be measured using an electron paramagnetic resonance (EPR) spectrometer. Alanine pellets are tissue equivalent, damage resistant, highly uniform ($\pm$ 2 mg), and facilitate reproducible dose measurements with overall uncertainty of less than 1%. Alanine/EPR dosimetry has been applied to measure radiation therapy level doses for mailed dosimetry audits.[39,40]

A PTW MP3-XS system (PTW Dosimetry, Freiburg, Germany) was used for detector placement in water and a PTW UNIDOS electrometer (PTW Dosimetry, Freiburg, Germany) was used for data collection for the diodes and chambers. The holders for alanine dosimeters were constructed at the National Research Council (NRC) of Canada, alanine pellets loaded into the holders and sealed at NRC, then carried to the ZAP-X facility by two of the co-authors (MM, BM). After irradiation, they were brought back to Canada for analysis.

2.4 | Absolute dose and output factor determination

In the general measurement setup (Figure 1), photon beams were directed vertically down toward the detector. The central axis of the detector was positioned either perpendicular to the central axis of the beam in the case of ion chambers, or parallel to the central axis of the beam in the case of diode or scintillation detectors, and submerged in the MP3-XS three-dimensional water tank at a depth of 7 mm. A depth of 7 mm was used because it corresponds to the depth of maximum dose for the ZAP-X system. The water tank was leveled using a precision digital level to be within $\pm$ 0.02° of the horizon and the setup alignment was periodically confirmed throughout the measurements. The exact arrangement, setup configuration, and measurement procedure were specific to each detector.

For the ion chamber measurements, both the original TG-51 and a TG-51 addendum protocol were followed for dose calibration and correction of the raw electrometer reading.[22,41] The polarity correction is generally small for MV photon beams but cannot be ignored for micro-chambers such as the A16.[42] Leakage currents can be a significant issue for chambers with very small volumes, and therefore, care was taken to ensure leakage was not a significant contributor to the measured signal.

For the W2 plastic scintillator, the Cherenkov light ratio (CLR) and system gain coefficient (G) must be determined through the manufacturer-recommended calibration procedure, and then used to obtain the Cherenkov-corrected detector signal.[43] The scintillator was read out using a MAX SD electrometer (Standard Imaging Inc., Middleton, Wisconsin, USA).

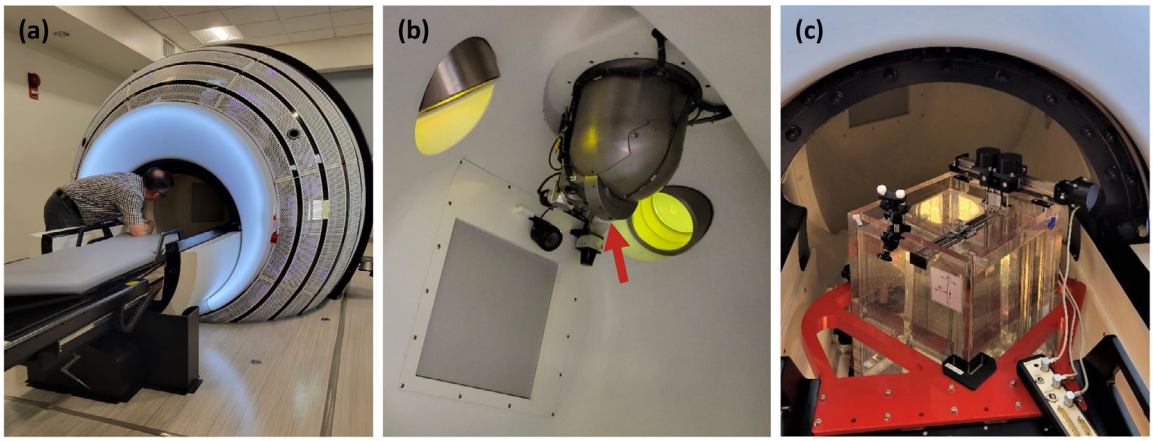

FIGURE 1 Photographs of the (a) ZAP-X system and (b) field-defining collimator (red arrow identifies one of the eight circular apertures). Also displayed are two observation windows and the flat panel kV detector. In panel (c), the general measurement setup is shown. A 3D water phantom specially designed for ZAP-X was mounted on the dedicated phantom holder (red bracket), aligned manually to the mechanical isocenter of the ZAP-X, and leveled through translation and rotation of the couch. A front pointer was used for isocenter location determination.

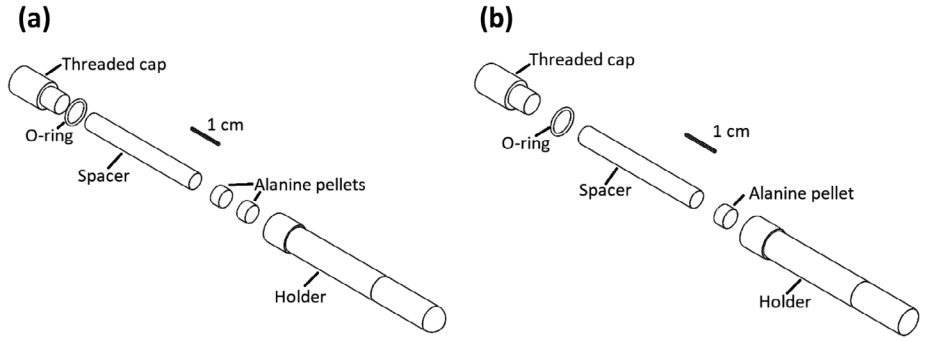

FIGURE 2 Deconstructed drawings of the alanine pellet holders, where the alanine pellets are inserted into the hollow portion labelled "Holder." Panel (a) shows the "Semiflex" alanine holder containing two alanine pellets, while panel (b) shows the "microSilicon" alanine holder containing one alanine pellet. On both panels, a 1 cm line indicates the scale. The midpoint of the alanine pellets is 7.5 mm from the end of the holder in (a) and the midpoint of the alanine pellet is 4.4 mm from the end of the holder in (b).

Alanine dosimeters consist of 60 mg alanine pellets (L-Alanine with 9.1% paraffin wax binder—Harwell Dosimeters, Oxfordshire, UK) in holders machined to mimic other detectors used in this work, such that the same methods for set-up and irradiation procedure can be applied for alanine dosimeters and other detectors. The waterproof alanine holders were machined from polyoxymethylene (POM, trade name Delrin) and have identical outer dimensions to the PTW Semiflex 31010 ionization chamber or the PTW microSilicon diode. Manufacturing drawings of the holders are shown in Figure 2. The "Semiflex" alanine holders contained two alanine pellets, while the "microSilicon" alanine holders contained one alanine pellet. Alanine dosimeters were irradiated to known doses close to 20 Gy. Ten "Semiflex" alanine holders (20 alanine pellets in total) were irradiated in separate set-ups with beams from the ZAP-X using the 25 mm collimator with the axis of the holders perpendicular to the beam axis. The point of measurement for these holders for all irradiations was the center of the alanine pellets, which is at the midpoint of the holder along the beam axis. Ten "microSilicon" alanine holders (ten alanine pellets in total) were irradiated in separate set-ups with beams from the ZAP-X using the 10 mm collimator with the axis of the holder parallel to the beam axis. The point of measurement for these holders was the center of the alanine pellets, which is 4.4 mm from the end of the holder along the beam axis. No correction for volume averaging was applied for the alanine dosimeters.

Absolute radiation output was measured multiple times during experiments using alanine dosimeters as well as the calibrated PTW Semiflex ion chamber. Validation measurements using alanine dosimeters were repeated 10 times for statistical uncertainty determination. The largest 25 mm diameter cone served as the reference field size. In addition, output for the 10 mm cone was also measured but due to its size, the alanine

dosimeter was not used for the smaller 7.5, 5, and 4 mm cones.

Alanine read out was performed using the NRC Bruker EMX spectrometer (Bruker Corporation, Billerica, Massachusetts, USA) with a high-sensitivity cavity (HS0105). The peak-to-peak amplitude of the EPR spectrum obtained for each irradiated alanine pellet was normalized by the mass of the pellet and corrected by subtracting the background of the signal for an unirradiated alanine pellet. The signal was normalized to the peak-to-peak intensity from the spectrum obtained from a fixed ruby to account for environmental fluctuations.

The dose delivered to the alanine pellets was determined using a calibration curve generated by irradiating alanine dosimeters from the same batch of alanine pellets used for the ZAP-X irradiations in the NRC cobalt-60 reference irradiator. Absorbed dose to water in the cobalt-60 beam is traceable to the NRC primary standard water calorimeter.[44] Doses between 15 and 800 Gy were delivered for calibration measurements. The alanine dosimeters were read out after a period of 48 h to ensure free radical production had stabilized.

To minimize the possibility of contamination or environmental effects, alanine pellets were loaded and hermetically sealed in the holders at NRC and carried to MedStar Georgetown University Hospital. Irradiated control alanine dosimeters were used to monitor the impact of travel on alanine dosimeters, as they went from Ottawa, Ontario, Canada, to the Washington, District of Columbia, USA area, and back. Four control dosimeters were irradiated to 20 Gy, one was irradiated to 15 Gy, and one was irradiated to 25 Gy. Two of the 20 Gy controls remained at NRC and the other four controls travelled with the alanine dosimeters to be irradiated in the ZAP-X beam. Read out of the control dosimeters was performed before and after sending alanine dosimeters.

Measurements performed using the diode and diamond detectors were perhaps the simplest to obtain and analyze as these require no additional corrections.

Field sizes were defined using circular collimators with diameter of 4, 5, 7.5, 10, 12.5, 15, 20, and 25 mm at 45 cm SAD. The 25 mm collimator served as the reference field size for absolute dose validation and for determining relative output factors. Reported output factors were calculated by averaging data over all measurements for that detector and field size. To ensure accurate detector positioning, the radiation-field center was determined by scanning the 10 mm field and repeated multiple times throughout the measurements.

2.5 | Uncertainties

Measurement uncertainties can be challenging to estimate in small-field dosimetry, but are essential for the proper interpretation of results.

TABLE 2 Uncertainty budget for NRC measurements of alanine dosimeters irradiated in the ZAP-X beam in terms of absorbed dose to water.

Component of uncertainty	Standard uncertainty (%)
Realization of reference dose (NRC primary standard)	0.4
Signal measurement—calibration	0.2
Environment effects—calibration	0.1
Mass of pellet	0.05
Spectrometer reproducibility	0.25
Calibration fit	0.35
Signal measurement—irradiation	0.20
Volume averaging	0.25
Energy dependence correction factor	0.35
Environment effects—irradiation[a]	0.2
Transportation of dosimeters[b]	0.25
Combined standard uncertainty (k = 1)	0.85

[a]Temperature at irradiation was supplied by CCI staff, an uncertainty of 0.3°C is assumed.
[b]Takes into account possible signal variation (e.g., due to environmental effects or free radical recombination).

TABLE 3 Uncertainty budget for dose determination following the modified TG-51 procedure using an ionization chamber calibrated in Co-60.

Component of uncertainty	Standard uncertainty (%)
SSD, depth, field setting	0.25
Signal measurement—M_{raw}	0.2
Correction factors—P_{TP}, P_{pol}, P_{ion}, P_{leak}	0.2
Volume averaging (P_{rp})	0.25
$N_{D,w}$ (ADCL)	0.75
k_Q	0.4
Assignment of k_Q	0.2
Stability of reference chamber	0.2
Beam stability during measurements	0.2
Combined standard uncertainty (k = 1)	1.02

Adapted from the TG-51 Addendum and valid for the 25 mm ZAP-X field.

2.5.1 | Absolute dose measurement

Table 2 shows the uncertainty in the absorbed dose to water obtained using alanine dosimeters and Table 3 shows the uncertainty in the absorbed dose to water obtained using an ionization chamber.

2.5.2 | Relative dose measurement

One can use Table 3 as a starting point for estimating uncertainties for relative measurements recognizing that, when comparing output factors, either for the same

TABLE 4 Cone output factors for five radiation detectors, including the microSilicon and microDiamond diode detectors, W2 plastic scintillator, A1SL thimble ion chamber, A16 micro ion chamber.

Cone diameter (mm)	Output factors				
	microSilicon	microDiamond	W2	A1SL	A16
4	0.749	0.739	0.736	–	–
5	0.824	0.818	0.809	–	–
7.5	0.910	0.914	0.899	–	–
10	0.946	0.949	0.942	0.913	–
12.5	0.965	0.966	0.962	0.951	0.951
15	0.976	0.977	0.975	0.971	0.961
20	0.990	0.991	0.990	0.99	0.981
25	1.000	1.000	1.000	1.000	1.000

detector for different field sizes, or for different detectors at the same field size, a number of components are common and therefore cancel (e.g., $N_{D,w}$, k_Q). At the same time, other components may increase in magnitude (e.g., volume averaging, beam stability). A reasonable uncertainty estimate for comparing output factors for different detectors is 0.4% and for comparing field sizes (same detector) the uncertainty is somewhat less, 0.3%.

3 | RESULTS

3.1 | Output factors

Table 4 shows radiation output factors obtained for the ZAP-X radiosurgical system. In total, 93 independent measurements were performed across all six detectors. Reported values for the microSilicon, microDiamond, and W2 detectors were averaged over five, one, and two sets of measurements at each field size, respectively. Output factors for the ionization chambers were determined for only field sizes of 10 to 25 mm (A1SL model) and 12.5 to 25 mm (A16 model).

Figure 3 displays output factor versus cone diameter for the different detector systems. The W2 scintillator yielded lower measurement variability as compared to the microSilicon diode. Specifically, output factor uncertainty for the W2 ranged from 0.1% (15 mm cone) to 0.14% (4 mm cone), whereas the range was 0.1% (20 mm cone) to 0.49% (5 mm cone) for the microSilicon.

Table 5 presents a comparison of output factors measured with the W2 versus those from the other detectors. Output factors agreed to within 1.8% between W2 and diodes for all the cone-shaped fields. The maximum deviation of 1.8% was between W2 and microSilicon at 5 mm field size. Percent differences in output factor were larger (0.4%–1.8%) at field sizes $\leq$ 7.5 mm and lower (0%–0.7%) for the field sizes $\geq$ 10 mm. Results for W2 and diode detectors exhibited an average difference in output factors of 0.6% over all field sizes. Larger differences were observed between the W2 and ion chambers. The greatest deviation occurred at 10 mm, where the measured output factor of A1SL was 3.2% lower as compared to W2.

3.2 | Absolute dose measurement and verification

For alanine dosimetry, measurements were averaged for ten repeated set-ups with the 10 and 25 mm cone sizes. Results for the intensity of the control alanine dosimeters were within 0.4%, independent of dose or whether the dosimeters stayed at NRC or traveled to the Washington, District of Columbia area, suggesting little impact of travel on the results obtained using alanine.

Since alanine measurements were obtained for two field sizes, it is possible to obtain an output factor and for the 10 mm field size this was comparable to results from the other detectors. For example, at 10 mm field size, output factors were 0.942 and 0.931 for the W2 and alanine dosimeter, respectively (1.2% difference). More important is the comparison of the dose measured using alanine with that obtained using a PTW 31010 ionization chamber. In the machine-specific reference field with a circular field size of 25 mm, the delivered dose (based on ion chamber) was 19.98 Gy, while the dose measured using alanine was 19.75 Gy, a difference of 1.2%. For the smaller field size of 10 mm, the dose delivered was 18.96 Gy, while the dose measured using alanine was 18.38 Gy, a difference of 3.1%.

4 | DISCUSSION

Stereotactic radiosurgery requires precisely targeted dose delivery to achieve optimal therapeutic response and minimize normal tissue complications. One of the

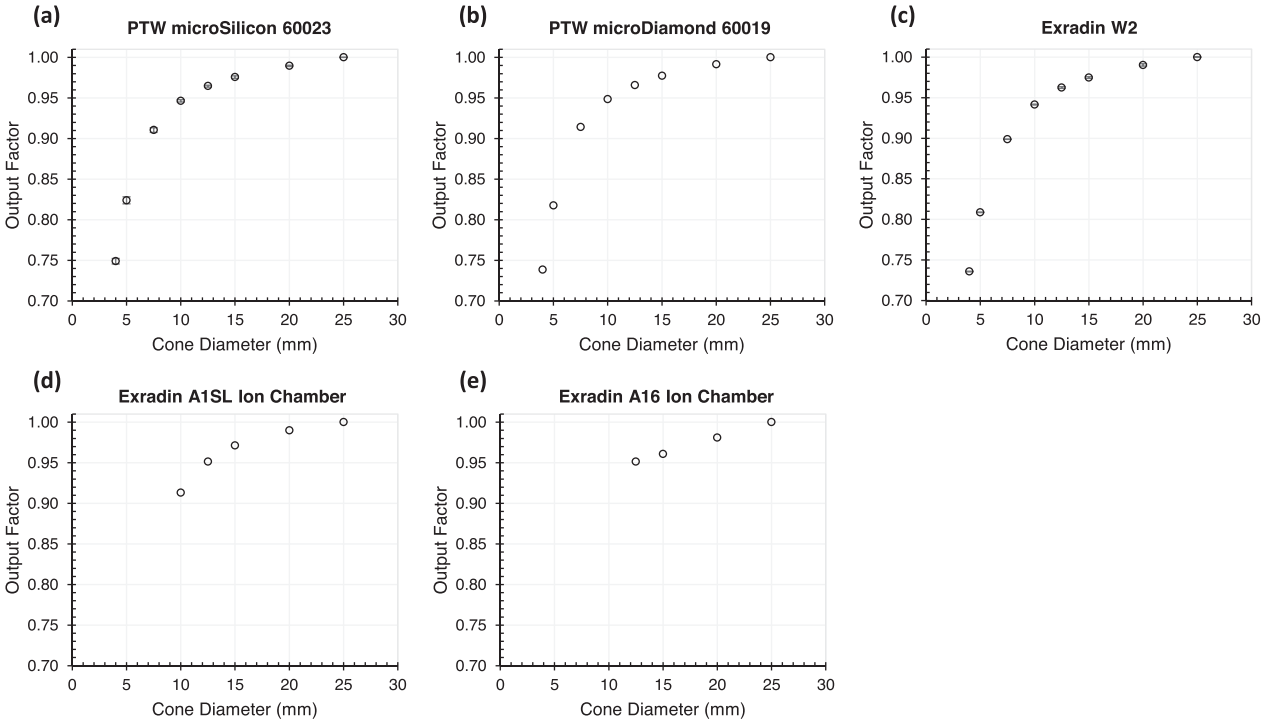

FIGURE 3 Output factors for the (a) microSilicon diode, (b) microDiamond detector, (c) W2 scintillator, (d) A1SL ion chamber, and (e) A16 ion chamber. Error bars in y-direction represent one standard deviation in the calculated output factor (note that some error bars are smaller than the symbol size).

TABLE 5 Percent difference in output factors measured with the W2 scintillator and other detectors.

Cone diameter (mm)	% Difference (W2 vs. microSilicon)	% Difference (W2 vs. microDiamond)	% Difference (W2 vs. A1SL)	% Difference (W2 vs. A16)
4	–1.7%	–0.4%	–	–
5	–1.8%	–1.1%	–	–
7.5	–1.2%	–1.6%	–	–
10	–0.4%	–0.7%	3.2%	–
12.5	–0.3%	–0.4%	1.2%	1.2%
15	–0.1%	–0.2%	0.4%	1.5%
20	0.0%	–0.1%	0.0%	0.9%
25	0.0%	0.0%	0.0%	0.0%

challenges for any SRS system lies in accurate determination of radiation output factors for small field sizes commonly employed in SRS treatment. Previous reports have documented general disagreement in the SRS community regarding output factors for field sizes $\leq$ 10 mm,[45] which may vary by ~35% based on detector.[46] These dosimetric uncertainties can propagate through the treatment planning system and impact gamma passing rates ($\pm$ 12.4%) measured by patient specific quality assurance depending on target size.[47] Therefore, it is critical to select a detector or detectors and a calibration protocol that facilitates accurate, reliable small field dosimetry measurements. The goal of this work was to assess radiation output factors for the novel ZAP-X radiosurgical unit using six commercially available dosimeters (Table 1).

The diodes and micro chambers used in this study cover the range of the commonly used detectors for absolute as well as relative dosimetry determination suitable for SRS systems. The consistent output factors for cones larger than 10 mm show their suitability for such field sizes. For cones less than 10 mm, only the diodes and W2 scintillator provided consistent output factor values, a result of their smaller size relative to the micro chambers. The micro chambers used in this study are some of the smallest ion chambers commercially

available and our results indicate the limitations of ion chambers in ultra small radiation fields.

Alanine dosimetry provided independent verification with direct traceability to primary standards. The alanine-derived absolute dose measurements had ± 0.85% uncertainty (see Table 2), compared to around 1% for the Semiflex ion chamber derived dose. The difference is mainly due to the different traceability of the two systems (NRC for the alanine, ADCL for the ion chamber). The agreement, therefore, of 1.2% for the absolute dose measured between chamber and alanine in the 25 mm reference field is well within combined uncertainties. The larger difference of 3.1% for the 10 mm field is outside the 95% confidence level for the combined uncertainties. However, the uncertainty budgets presented in Tables 2 and 3 are for the machine-specific reference field. Uncertainties will be larger for the smaller 10 mm field because volume averaging will play a larger role given the relatively large size of the alanine dosimeters and the simplified TG-51 procedure used with the Semiflex ion chamber.[48] Further investigation with smaller alanine dosimeters, to reduce volume averaging, is warranted. In addition, an accurate determination of the k_Q factor for the 2.7 MV photon beam of the ZAP-X system, as well as clinical reference dosimetry utilizing TG-155 or TRS-483 protocols, will also be valuable.

Previously, a few other groups have published small field dosimetry data with applications to radiosurgery. For CyberKnife system, Al Kafi et al. concluded micro-ionization chambers, diodes, and scintillators are suitable for small field output factor measurements,[20] whereas Francescon et al. demonstrated variations in output factors up to 9%, as measured by microchambers.[49] For the ZAP-X system, Weidlich et al. showed that peripheral dose fall-off measurements depend on the type of detector used (e.g., microSilicon diode, microDiamond, film, etc.),[28] while Sorensen et al. determined a modified TG-51 protocol is ideal for absolute dose measurements, although water tank setup is challenging due to limited space inside the treatment unit.[26] Meanwhile, Pinnaduwage et al. showed minimal differences in beam data collected with three different diodes (PTW 60012 Diode E, PTW 60018 SRS Diode, and Sun Nuclear EDGE).[27] Given these findings, continued development of practical guidelines for ZAP-X clinical dosimetry is imperative.

Agreement between the diodes, scintillator, ionization chambers, and alanine dosimeter (Table 4) is consistent with generalized small field output factor measurements reported by other groups. For example, Jacqmin et al. investigated application of the Exradin W2 and IBA RAZOR Diode Detector to SRS small field dosimetry.[50] The two detectors yielded output factors that agreed within 1.3%–1.8% across the range of measured field sizes (MLC-defined field sizes of 1×1 cm^2 to 3×3 cm^2, as well as fixed cone-defined field sizes of 4 –17.5 mm diameter). Furthermore, Al Kafi et al. demonstrated that PTW Diode (TM 60016), PTW Diamond (TM 60003), Exradin W1, and Exradin W2 detectors produced output factors with 1%–2% differences for nominal cone sizes between 0.5 and 5.0 cm.[20] In that study, the measured data were in good agreement with Monte Carlo simulated field output factors. Each radiation detection system that measures dosimetric parameters for small fields has advantages and limitations. Diode detectors have high spatial resolution due to their small size, but exhibit dependence on the incident energy and dose rate. Diamond detectors are compact and water equivalent, although O'Brien et al. noted the PTW microDiamond over-responds to small radiation fields resulting in biased correction factors.[51] Despite favorable dose response linearity of ionization chambers, their relatively large active volume usually limits utility for small field measurements. Plastic scintillators provide superior spatial resolution with no dependence on energy, temperature, or dose rate; however, scintillation systems require sophisticated calibrations to remove Cherenkov radiation and have an accumulated dose dependence due to radiation damage of the sensitive material.[36–38] Alanine dosimeters are tissue equivalent and enable absolute dosimetry, although EPR readout equipment is expensive and rarely available in most facilities. In addition, the relatively large size of the alanine dosimeter may limit its suitability to fields less than 10 mm.

In this study, the microSilicon diode, microDiamond detector, and W2 scintillator yielded output factors for all cone sizes (4 —25 mm) (Table 4). The A1SL and A16 ionization chambers provided output factors at 10 —25 mm and 12.5 —25 mm, respectively. We did not use the A1SL and A16 ion chambers to measure fields < 10 mm in diameter due to unreliable setup and volume averaging effects. Alanine dosimetry allowed dose measurements for the 10 mm collimator and 25 mm reference cone. All detectors produced consistent output factors within statistically acceptable variations at field sizes greater than 10 mm (Figure 1). For fields less than 10 mm in diameter, the microSilicon, microdiamond, and W2 produced consistent data. The larger output factors obtained using the diodes compared to the W2 may be due to over-response of diode detectors at small field sizes. Furthermore, larger discrepancies at the smallest field sizes (≤ 7.5 mm) may be related to detector alignment, perturbation effects, and/or the lack of charge particle equilibrium.

5 | CONCLUSION

This is the first study that used six types of detectors to characterize small field output factors for the ZAP-X radiosurgery system. Our results demonstrate that the PTW microSilicon, PTW microDiamond, and Exradin W2 are suitable for output factor determinations in fields

as small as 4 mm in diameter. The A1SL ion chamber, A16 microchamber, and alanine dosimeter were better suited for measurements in field sizes of 10 mm or larger. Agreement among devices is consistent with the findings of other groups. Lower measurement variability with the W2 plastic scintillator may indicate it has more reliable performance than the popularly used microSilicon diode. Alanine measurements also provided an independent method of validating the dose determined using a calibrated ion chamber, with the results for the largest reference field showing very good agreement consistent with the measurement uncertainty of 1.3%.

ACKNOWLEDGMENTS

The authors thank Mark Shinn and Nero Henderson at ZAP-X for their assistance in setting up the water tank and operating the machine to facilitate the measurements. The authors thank Dr. Robert Chatelain of NRC for performing the EPR spectrometer readout of the alanine dosimeters and Jean Desserault of NRC for manufacturing the alanine holders used for this work.

CONFLICT OF INTEREST STATEMENT

The authors have no relevant conflicts of interest to disclose.

REFERENCES

1. O'Beirn M, Benghiat H, Meade S, et al. The expanding role of radiosurgery for brain metastases. *Medicines (Basel)*. 2018;5(3):90. doi:10.3390/medicines5030090. Published 2018 Aug 14.
2. Soliman H, Das S, Larson DA, Sahgal A. Stereotactic radiosurgery (SRS) in the modern management of patients with brain metastases. *Oncotarget*. 2016;7(11):12318-12330. doi:10.18632/oncotarget.7131
3. Kirkpatrick JP, Soltys SG, Lo SS, Beal K, Shrieve DC, Brown PD. The radiosurgery fractionation quandary: single fraction or hypofractionation. *Neuro Oncol*. 2017;19:ii38-ii49. doi:10.1093/neuonc/now301. suppl_2.
4. Harris L, M Das J. Stereotactic radiosurgery. In: *StatPearls*. Treasure Island (FL): StatPearls Publishing; July 25, 2023.
5. Patil CG, Pricola K, Sarmiento JM, Garg SK, Bryant A, Black KL. Whole brain radiation therapy (WBRT) alone versus WBRT and radiosurgery for the treatment of brain metastases. *Cochrane Database Syst Rev*. 2017;9(9):CD006121. doi:10.1002/14651858.CD006121.pub4. Published 2017 Sep 25.
6. Xue J, Kubicek GJ, Grimm J, et al. Biological implications of whole-brain radiotherapy versus stereotactic radiosurgery of multiple brain metastases. *J Neurosurg*. 2014:60-68. doi:10.3171/2014.7.GKS141229. 121 Suppl
7. Patel KR, Burri SH, Boselli D, et al. Comparing pre-operative stereotactic radiosurgery (SRS) to post-operative whole brain radiation therapy (WBRT) for resectable brain metastases: a multi-institutional analysis. *J Neurooncol*. 2017;131(3):611-618. doi:10.1007/s11060-016-2334-3
8. St Clair WH, Given CA. Stereotactic radiosurgery associated neurotoxicity. *Technol Cancer Res Treat*. 2003;2(2):147-152. doi:10.1177/153303460300200211
9. Kotecha R, Gondi V, Ahluwalia MS, Brastianos PK, Mehta MP. Recent advances in managing brain metastasis. *F1000Res*. 2018;7. doi:10.12688/f1000research.15903.1. F1000 Faculty Rev-1772. Published 2018 Nov 9.
10. Cohen-Inbar O, Sheehan JP. The role of stereotactic radiosurgery and whole brain radiation therapy as primary treatment in the treatment of patients with brain oligometastases—a systematic review. *J Radiosurg SBRT*. 2016;4(2):79-88.
11. Szeifert G, Levivier M, Kondziolka D, Lunsford D, Brotchi J, Nyáry I. Sugár agysebészet a XXI. Század hajnalán: a gamma-kés C-modell automata pozícionáló robot rendszerrel [Radiosurgery of the brain at the beginning of the 21st century: gamma knife with C-table]. *Orv Hetil*. 2001;142(40):2181-2192.
12. Friedman WA, Bova FJ. The University of Florida radiosurgery system. *Surg Neurol*. 1989;32(5):334-342. doi:10.1016/0090-3019(89)90135-3
13. Kandasamy R, Kiat SS, Ruzman N. An innovative modification of an old radiosurgery system. *Malays J Med Sci*. 2013;20(5):90-91.
14. Nath SK, Lawson JD, Wang JZ, et al. Optically-guided frameless linac-based radiosurgery for brain metastases: clinical experience. *J Neurooncol*. 2010;97(1):67-72. doi:10.1007/s11060-009-9989-y
15. Oh SA, Park JW, Yea JW, Kim SK. Evaluations of the setup discrepancy between BrainLAB 6D ExacTrac and cone-beam computed tomography used with the imaging guidance system Novalis-Tx for intracranial stereotactic radiosurgery. *PLoS One*. 2017;12(5):e0177798. doi:10.1371/journal.pone.0177798. Published 2017 May 19.
16. Ding C, Saw CB, Timmerman RD. Cyberknife stereotactic radiosurgery and radiation therapy treatment planning system. *Med Dosim*. 2018;43(2):129-140. doi:10.1016/j.meddos.2018.02.006
17. Gersh JA, Willett B. Determination of kQ using MLC-collimated rectangular fields for absolute dosimetry of the CyberKnife. *J Appl Clin Med Phys*. 2015;16(6):273-280. doi:10.1120/jacmp.v16i6.5720. Published 2015 Nov 8.
18. Weidlich GA, Schneider MB, Adler JR. Self-shielding analysis of the Zap-X system. *Cureus*. 2017;9(12):e1917. doi:10.7759/cureus.1917. Erratum in: Cureus. 2019 May 17;11(5):c22.
19. Weidlich GA, Bodduluri M, Achkire Y, Lee C. Characterization of a novel 3 megavolt linear accelerator for dedicated intracranial stereotactic radiosurgery. *Cureus*. 2019;11(3):e4275. doi:10.7759/cureus.4275. Published 2019 Mar 19.
20. Al Kafi MA, Arib M, Al Moussa A, et al. Small field output factor measurement and verification for CyberKnife robotic radiotherapy and radiosurgery system using 3D polymer gel, ionization chamber, diode, diamond and scintillator detectors, Gafchromic film and Monte Carlo simulation. *Appl Radiat Isot*. 2023;192:110576. doi:10.1016/j.apradiso.2022.110576
21. Paul JM, Koch RF, Philip PC. AAPM Task Group 21 protocol: dosimetric evaluation. *Med Phys*. 1985;12(4):424-430. doi:10.1118/1.595704
22. Almond PR, Biggs PJ, Coursey BM, et al. AAPM's TG-51 protocol for clinical reference dosimetry of high-energy photon and electron beams. *Med Phys*. 1999;26(9):1847-1870. doi:10.1118/1.598691
23. Das IJ, Francescon P, Moran JM, et al. Report of AAPM Task Group 155: megavoltage photon beam dosimetry in small fields and non-equilibrium conditions. *Med Phys*. 2021;48(10):e886-e921. doi:10.1002/mp.15030
24. INTERNATIONAL ATOMIC ENERGY AGENCY. Absorbed Dose Determination in External Beam Radiotherapy, Technical Reports Series No. 398, IAEA, Vienna (2000).
25. Palmans H, Andreo P, Huq MS, Seuntjens J, Christaki KE, Meghzifene A. Dosimetry of small static fields used in external photon beam radiotherapy: summary of TRS-483, the IAEA-AAPM international Code of Practice for reference and relative dose determination. *Med Phys*. 2018;45(11):e1123-e1145. doi:10.1002/mp.13208
26. Sorensen SP, Jani SS, Pinnaduwage DS, Yan X, Srivastava SP. Technical note: absolute dose measurements of a vault-free radiosurgery system. *Med Phys*. 2022;49(12):7733-7741. doi:10.1002/mp.15912

27. Pinnaduwage DS, Srivastava SP, Yan X, et al. Small-field beam data acquisition, detector dependency, and film-based validation for a novel self-shielded stereotactic radiosurgery system. *Med Phys*. 2021;48(10):6121-6136. doi:10.1002/mp.15091
28. Weidlich GA, Chung W, Kolli S, Thirunarayanan I, Loysel T. Characterization of the ZAP-X® peripheral dose fall-off. *Cureus*. 2021;13(3):e13972. doi:10.7759/cureus.13972
29. Khan FM. *Physics of radiation therapy*. 4th edition. Lippincott Williams & Wilkins; 2010.
30. Lárraga-Gutiérrez JM, Ballesteros-Zebadúa P, Rodríguez-Ponce M, García-Garduño OA, de la Cruz OO. Properties of a commercial PTW-60019 synthetic diamond detector for the dosimetry of small radiotherapy beams. *Phys Med Biol*. 2015;60(2):905-924. doi:10.1088/0031-9155/60/2/905
31. Georgiou G, Kumar S, Würfel JU, et al. The PTW microSilicon diode: performance in small 6 and 15 MV photon fields and utility of density compensation. *Med Phys*. 2021;48(12):8062-8074. doi:10.1002/mp.15329
32. Damodar J, Odgers D, Pope D, Hill R. A study on the suitability of the PTW microDiamond detector for kilovoltage x-ray beam dosimetry. *Appl Radiat Isot*. 2018;135:104-109. doi:10.1016/j.apradiso.2018.01.025
33. Le Roy M, de Carlan L, Delaunay F, et al. Assessment of small volume ionization chambers as reference dosimeters in high-energy photon beams. *Phys Med Biol*. 2011;56(17):5637-5650. doi:10.1088/0031-9155/56/17/011
34. Muir BR. Ion chamber absorbed dose calibration coefficients, N(D,w), measured at ADCLs: distribution analysis and stability. *Med Phys*. 2015;42(4):1546-1554. doi:10.1118/1.4914381
35. Martin-Martin G, Aguilar PB, Barbés B, Guibelalde E. Assessment of ion recombination correction and polarity effects for specific ionization chambers in flattening-filter-free photon beams. *Phys Med*. 2019;67:176-184. doi:10.1016/j.ejmp.2019.07.018
36. Thrower S, Prajapati S, Holmes S, Schüler E, Beddar S. Characterization of the plastic scintillator detector system Exradin W2 in a high dose rate flattening-filter-free photon beam. *Sensors (Basel)*. 2022;22(18):6785. doi:10.3390/s22186785. Published 2022 Sep 8.
37. Beddar AS, Mackie TR, Attix FH. Water-equivalent plastic scintillation detectors for high-energy beam dosimetry: iI. Properties and measurements. *Phys Med Biol*. 1992;37(10):1901-1913. doi:10.1088/0031-9155/37/10/007
38. Archambault L, Arsenault J, Gingras L, Sam Beddar A, Roy R, Beaulieu L. Plastic scintillation dosimetry: optimal selection of scintillating fibers and scintillators. *Med Phys*. 2005;32(7Part1):2271-2278. doi:10.1118/1.1943807
39. Sharpe PHG, Sephton JP. Alanine dosimetry at NPL—the development of a mailed reference dosimetry service at radiotherapy dose levels. In: IAEA-SM-356/R6 Proc. International symposium on techniques for high dose dosimetry in Industry, Agriculture and Medicine, 2–5 November 1998, Vienna. 1998.
40. Mansour I. *Development of mailed dosimetric audit for external beam radiation therapy using alanine dosimeters*. Diss., Carleton University; 2018.
41. McEwen M, DeWerd L, Ibbott G, et al. Addendum to the AAPM's TG-51 protocol for clinical reference dosimetry of high-energy photon beams. *Med Phys*. 2014;41(4):041501. doi:10.1118/1.4866223
42. Miller JR, Hooten BD, Micka JA, DeWerd LA. Polarity effects and apparent ion recombination in microionization chambers. *Med Phys*. 2016;43(5):2141. doi:10.1118/1.4944872
43. Galavis PE, Hu L, Holmes S, Das IJ. Characterization of the plastic scintillation detector Exradin W2 for small field dosimetry. *Med Phys*. 2019;46(5):2468-2476. doi:10.1002/mp.13501
44. Seuntjens JP, Ross CK, Shortt KR, Rogers DW. Absorbed-dose beam quality conversion factors for cylindrical chambers in high energy photon beams. *Med Phys*. 2000;27(12):2763-2779. doi:10.1118/1.1328081
45. Tsai JS, Rivard MJ, Engler MJ, Mignano JE, Wazer DE, Shucart WA. Determination of the 4 mm Gamma Knife helmet relative output factor using a variety of detectors. *Med Phys*. 2003;30(5):986-992. doi:10.1118/1.1567736
46. Haryanto F, Fippel M, Laub W, Dohm O, Nüsslin F. Investigation of photon beam output factors for conformal radiation therapy–Monte Carlo simulations and measurements. *Phys Med Biol*. 2002;47(11):N133-N143. doi:10.1088/0031-9155/47/11/401
47. Lechner W, Primeßnig A, Nenoff L, Wesolowska P, Izewska J, Georg D. The influence of errors in small field dosimetry on the dosimetric accuracy of treatment plans. *Acta Oncol*. 2020;59(5):511-517. doi:10.1080/0284186X.2019.1685127
48. Low DA, Parikh P, Dempsey JF, Wahab S, Huq S. Ionization chamber volume averaging effects in dynamic intensity modulated radiation therapy beams. *Med Phys*. 2003;30(7):1706-1711. doi:10.1118/1.1582558
49. Francescon P, Kilby W, Satariano N, Orlandi C, Elshamndy S. The impact of inter-unit variations on small field dosimetry correction factors, with application to the CyberKnife system. *Phys Med Biol*. 2019;64(3):035006. doi:10.1088/1361-6560/aaf971. Published 2019 Jan 22.
50. Jacqmin DJ, Miller JR, Barraclough BA, Labby ZE. Commissioning an Exradin W2 plastic scintillation detector for clinical use in small radiation fields. *J Appl Clin Med Phys*. 2022;23(8):e13728. doi:10.1002/acm2.13728
51. O'Brien DJ, León-Vintró L, McClean B. Small field detector correction factors kQclin,Qmsr (fclin,fmsr) for silicon-diode and diamond detectors with circular 6 MV fields derived using both empirical and numerical methods. *Med Phys*. 2016;43(1):411. doi:10.1118/1.4938584

How to cite this article: Jermain PR, Muir B, McEwen M, Niu Y, Pang D. Accurate machine-specific reference and small-field dosimetry for a self-shielded neuro-radiosurgical system. *Med Phys*. 2024;51:4423–4433. https://doi.org/10.1002/mp.17111